

Hydrolysis of N₂O₅ on Submicron Sulfuric Acid Aerosols

Mattias Hallquist, David J. Stewart, Jacob Baker,[†] and R. Anthony Cox*

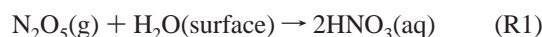
Centre for Atmospheric Science, Department of Chemistry, University of Cambridge, Lensfield Road, Cambridge CB2 1EW, U.K.

Received: November 8, 1999; In Final Form: February 14, 2000

The kinetics of reactive uptake of gaseous N₂O₅ on submicron sulfuric acid aerosol particles has been investigated using a laminar flow reactor coupled with a differential mobility analyzer (DMA) to characterize the aerosol. The particles were generated by homogeneous nucleation of SO₃/H₂O mixtures. In the H₂SO₄ concentration range 26.3–64.5 wt % the uptake coefficient was $\gamma = 0.033 \pm 0.004$, independent of acid strength. For an acid strength of 45 wt % γ was found to decrease with increasing temperature over the range 263–298 K. From this, temperature dependence values of -115 ± 30 kJ/mol and -25.5 ± 8.4 J/K mol were determined for the changes in enthalpy and entropy of the uptake process, respectively. The results are consistent with a previous model of N₂O₅ hydrolysis involving both a direct and an acid catalyzed mechanism, with uptake under the experimental conditions limited by mass accommodation.

Introduction

It is now well-known that hydrolysis of N₂O₅ on the surfaces of aerosol particles and cloud droplets is the dominant removal channel for nitrogen oxides at night. It is therefore important in determining the oxidative capacity of the atmosphere as the concentrations of NO_x strongly influence the rate of tropospheric ozone formation.



Reaction R1 converts reactive nitrogen oxide species (NO_x) into the longer-lived reservoir species HNO₃, which is then removed from the atmosphere via wet or dry deposition. It has been shown by Dentener and Crutzen¹ that the inclusion of this reaction in a global tropospheric model, assuming an uptake coefficient of 0.1 on ammonium hydrogen sulfate aerosol, decreases the NO_x and O₃ levels by 45% and 10% with respect to values obtained by considering only gas-phase chemistry in the summertime at mid-latitudes (45° N, 500 hPa, mid-June). Even larger relative changes are predicted for higher latitudes and in the planetary boundary layer. This reaction is also important in the stratosphere, a fact that was illustrated after the eruption of Mount Pinatubo. The NO_x levels in the stratosphere were significantly depleted due to hydrolysis of N₂O₅ on the large quantity of sulfuric acid aerosol generated by the volcanic gases.² The reactive uptake coefficient of N₂O₅ is dependent on the characteristics of the aerosol such as the particle surface to gas volume ratio, the chemical composition of the aerosol, and the corresponding reactivity of N₂O₅ on the surface.³

A major source of uncertainty in model estimates of the impact of heterogeneous reactions is the lack of certainty in the values used for the uptake coefficients. In the recent past, the hydrolysis of N₂O₅ with H₂SO₄/H₂O aerosol particles has been studied in detail under stratospheric conditions, i.e. concentrated H₂SO₄ (50–80 wt %) at low temperature (185–

260 K), but there is less information for tropospheric conditions. There is also some disagreement as to the effect of relative humidity, i.e., the acid strength of the aerosol, on the uptake coefficient. Hu and Abbatt⁴ present results in which the uptake coefficient shows a tendency to decrease with increasing humidity (decreasing acid strength) over the range 8.5–90%, whereas the model developed by Robinson et al.,⁵ based on literature data and their studies of uptake onto large droplets and bulk surfaces, predicts only a very slight increase of the rate of uptake as the acid strength is raised. The motivation of this study was therefore 2-fold. First to determine the rate of uptake of N₂O₅ on sulfuric acid aerosol under tropospheric conditions and second to compare our data to that of Hu and Abbatt⁴ and Robinson et al.⁵ to confirm whether or not the uptake is dependent on the acid strength of the aerosol.

In this study the uptake of N₂O₅ on sulfuric acid aerosols was measured over a wide range of acid concentrations (26.3–64.5 wt %) at room temperature corresponding to a relative humidity (RH) range of 8–80%. The temperature dependence of the uptake was determined over the range 263–298 K for an acid concentration of 45 wt %. Since these measurements have been taken over a wide range of relative humidity, they allow a reliable assessment of the dependence of the reactive uptake coefficient on the water content of the aerosol. The resulting relative humidity and temperature dependences are discussed. Comparisons of these results are made with preexisting models of the uptake of gaseous species on aerosol particles.

The use of submicron aerosol particles for these studies has two advantages. The first is to minimize the effects of gas-phase diffusion to the acid surface on the uptake rates, which can be a problem when bulk surfaces are used. Second the sulfuric acid present in the atmosphere is contained in small particles such as these, so the experiment is a better representation of what is actually occurring in the atmosphere.

Experimental Section

Uptake coefficients of N₂O₅ on sulfuric acid aerosol particles were determined using a recently built aerosol flow tube system described by Baker et al.⁶ The system described in that paper

* To whom correspondence should be addressed. E-mail: rac26@cam.ac.uk.

[†] Present address: School of Sciences, University of Sunderland, Benedict Building, St. George's Way Sunderland SR2 7BW, U.K.

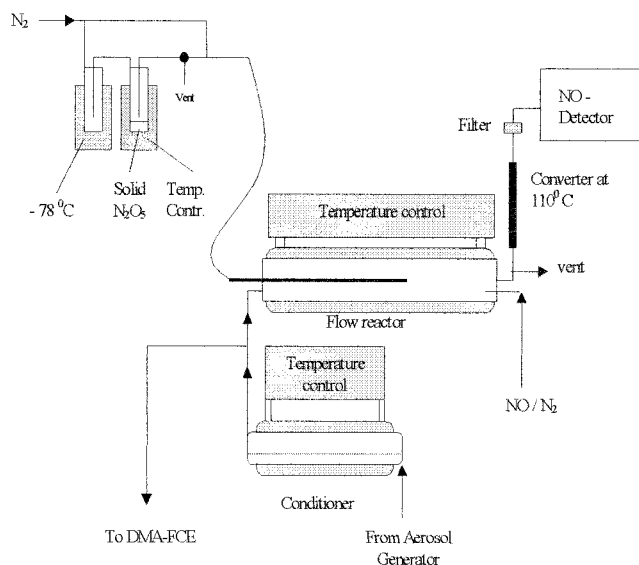


Figure 1. Schematic diagram of the flow tube system. Shaded areas are temperature controlled.

has been modified, and a schematic diagram of the revised system is shown in Figure 1. Four main subsystems connected to the flow tube are aerosol generation, aerosol characterization, N₂O₅ delivery, and the detection system. These will be described in turn.

Aerosol Generation. The sulfuric acid aerosol generator is based on the homogeneous nucleation of SO₃ and water. Sulfur trioxide was entrained into a filtered nitrogen stream (MG Gases) by passing the nitrogen over fuming sulfuric acid (BDH, 30% SO₃). The sulfur trioxide laden gas stream was then injected axially into a nucleation chamber where it came into contact with a sheath flow of humidified nitrogen. Sulfuric acid particles were produced upon mixing and formed a column of particles down the chamber. On exiting the nucleation chamber, the aerosol entered a 250 mL round-bottomed flask, where it was diluted with a further flow of humidified nitrogen and mixed with a Teflon coated magnetic stirrer to ensure the aerosol particles were homogeneously distributed in the gas stream. The product from this system is a stable aerosol under a specifically chosen condition, i.e., RH and temperature. The relative humidities in the aerosol generation system were monitored using Humitter 50Y probes (Vaisala) which have a precision of ca. ±2%. On exiting the aerosol generation system, the aerosol flow is sent to a switching valve which diverts it either to the reaction cell or to a vent. If the aerosol is directed to the vent, the flow is replaced by an equal bypass flow of humidified nitrogen. Before entering the cell the flow is passed through two Pyrex glass conditioners. The first (3 cm i.d., 55 cm length) containing a bulk solution of sulfuric acid at the appropriate concentration, which is used to fine-tune the concentration of the aerosol. The relative humidity is controlled by the equilibrium vapor pressure of water above the sulfuric acid solution. The next conditioner (3.5 cm i.d., 60 cm length) was used to precool the aerosol particles when working at lower temperatures. After the two conditioning flow tubes, the aerosol was divided into two flows. A flow of 2800 cm³(STP) min⁻¹ was directed to the differential mobility analyzer (DMA) and a flow of 1000 cm³(STP) min⁻¹ directed into the flow reactor (3.2 cm i.d. and 80 cm length). In this way the aerosol characteristics could be monitored during the course of an experiment. From the aerosol characterization it was found that the aerosol generator takes approximately 1 h to stabilize after setting the flows. After this time the particle number density remained

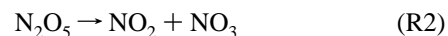
constant to within ±7% over the time of a kinetic run (ca. 1/2 – 1 h). The aerosol surface area typically varied by less than 10% over the same period.

Aerosol Characterization. The aerosol was characterized using a differential mobility analyzer (DMA) (Hauke EMS VIE-08) with a Faraday cup electrometer serving as the detector. The DMA output is a number density per size channel with software corrections made for the fraction of particles charged, the slip factor, and the effects of multiple charging. The working range of the DMA was set up to measure particle radii of 0.02–0.5 μm, with measurements being made at 35 selected size channels over 5 min. The characterization of the aerosol using the DMA was compared to the method using UV spectroscopy and particle counting as were used in a previous study.⁶ The difference in measured surface area was less than 5% between these methods. However, the DMA is easier to use and has a lower detection limit, and hence the DMA was used to characterize the aerosol in all kinetic measurements. Since most of the experiments were done at high relative humidity, the sheath air flow in the DMA was humidified to match the relative humidity of the aerosol flow to prevent the aerosol particle sizes from changing during sampling.

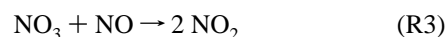
For the low-temperature data, corrections were made to the measured aerosol surface area to take into account the difference in temperature and, hence, relative humidity in the flow tube and the DMA. Thermodynamic data derived from Perry and Green⁷ were used.

N₂O₅ Delivery System. N₂O₅ was synthesized prior to use by mixing NO and excess O₃, in a flow system. The N₂O₅ produced was trapped and stored at 195 K. In the delivery system the solid N₂O₅ was held in a cold trap at 240 K, and a slow flow of dried nitrogen gas was used to entrain the N₂O₅. This flow could either be directed to the flow system or to the vent and was pre-diluted with additional nitrogen to give a total flow of about 50 cm³(STP) min⁻¹ of N₂O₅. This mixture was delivered to the aerosol flow tube by means of a sliding stainless steel injector. The N₂O₅ stream was passed through the inside of the injector using a 1/8 in. Teflon tube. The end of the injector is fitted with a Teflon “pepper pot” to enhance the mixing of this stream with the aerosol. To minimize the effects of wall loss, the interior surface of the flow reactor was coated with halocarbon wax.

N₂O₅ Detection. N₂O₅ was detected at the exit of the flow tube by titration with NO.⁸ A flow of 30 cm³(STP) min⁻¹ of a mixture of 30 ppm NO in nitrogen (Messer) was used, giving an NO concentration of approximately 700 ppb. NO was added contra flow to the main gas stream at the end of the flow tube. On exiting the flow tube, the sample gas stream passed through a heated glass tube, where the N₂O₅ thermally decomposes:



The NO₃ produced is then titrated with the excess NO to produce NO₂:



The amount of N₂O₅ at the exit of the flow tube can therefore be obtained by measuring the change in concentration of NO when the N₂O₅ stream is switched on and off. NO was detected by means of a commercial nitrogen oxides monitor (Monitor Labs model 8440). This detector has a sampling flow rate of 450 cm³(STP) min⁻¹ and can measure NO concentrations up to 1 ppm. The detection limit of the instrument was 5 ppb (1.25 × 10¹¹ cm⁻³) with a S/N = 2. The change in NO was shown to

TABLE 1: Aerosol Characteristics and Concentrations Used in the Experiments

no. (cm ⁻³)	(1.5–4) × 10 ⁵
area (cm ² /cm ³)	(1.8–15) × 10 ⁻⁴
vol (cm ³ /cm ³)	(6.5–100) × 10 ⁻¹⁰
peak radius (nm)	120–220
RH (%)	8–80
[H ₂ SO ₄] (wt %)	26.3–64.5
[N ₂ O ₅] (molecules/cm ³)	(2.5–12.5) × 10 ¹²

be a linear function of the flow rate through the N₂O₅ trap. To prevent damage to the analyzer, a filter removing particulate matter was fitted in the sample line. Nitric acid produced in the reaction was removed by using nylon tubing, which adsorbs HNO₃ between the exit of the flow tube and the NO detector. Both the filter and the nylon tubing are inert to NO, so the concentrations of NO were not affected. NO₂ present in the gas stream did not interfere with the NO measurements.

Procedure. The flows entering the reaction chamber from the aerosol generator were set so that the total flow was 3.8 sLpm. The DMA sampled 2800 cm³(STP) min⁻¹ leaving a flow of 1000 cm³(STP) min⁻¹ of the aerosol flow to enter the reaction chamber. Under these conditions the flow in the tube is laminar and well-developed at 99% of the final velocities after about 2 cm.⁹ The time for diffusional mixing is estimated to be about 5 s, assuming a diffusion coefficient of 0.1 cm²/s for N₂O₅ in air as calculated by Hu and Abbatt.⁴ No data were taken in this mixing region, which corresponded to the first 10 cm after the N₂O₅ inlet.

The characteristics of the aerosol and the concentrations used in the experiments are summarized in Table 1. The experimental procedure was to determine a first-order loss of N₂O₅ by changing the position of the sliding injector to vary the contact time (20–45 s) between the aerosol and the N₂O₅ and monitoring the change in N₂O₅ concentration. The aerosol flow was switched out of the cell before and after each kinetic run, and an experiment carried out in the absence of aerosol in order to discriminate between N₂O₅ wall loss and N₂O₅ loss to the aerosol. The rate constant for reaction with and without aerosol present, obtained from the slope of a plot of ln[N₂O₅] against contact time, was then corrected for non-plug-flow conditions. First the observed wall loss rate constant was corrected for the effect of diffusion to the walls on the concentration of N₂O₅ by solution of the diffusion equation with first-order kinetics as described by Brown.¹⁰ Appropriate values of the flow velocity, diffusion coefficient, radius of the flow tube, and the measured wall loss were used. The correction of the observed decay rate coefficient in the presence of aerosol for the effects of wall loss under non-plug-flow conditions was then made by an iterative procedure also described in the paper by Brown.¹⁰ The diffusion equation was solved for appropriate values of the corrected wall loss for the same conditions, the diffusion coefficient, radius of the flow tube, and flow velocity. The uncorrected rate coefficient was multiplied by 1.2 and entered as a “first guess” in the iteration process. The reactive uptake coefficient, γ , was then calculated from this final corrected rate coefficient, k , using eq 1, where A is the surface area of the aerosol per unit volume

$$k = A \left(\frac{a}{D_{\text{N}_2\text{O}_5}} + \frac{4}{\langle c \rangle \gamma} \right) \quad (1)$$

of carrier gas (cm⁻¹), a is the radius of the particles (cm), $D_{\text{N}_2\text{O}_5}$ is the diffusion coefficient for N₂O₅ in nitrogen (cm² s⁻¹), and $\langle c \rangle$ is the average speed of the gas molecules (cm s⁻¹). The calculated γ obtained using eq 1 was found not to be significantly different from that calculated using the more

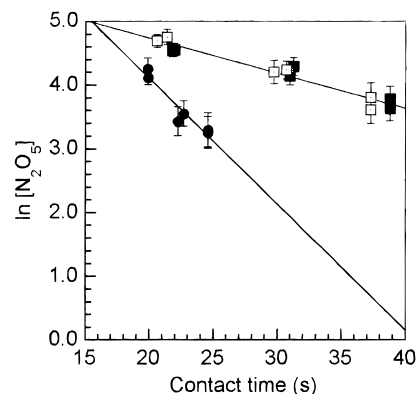


Figure 2. An example of a ln [N₂O₅] vs contact time plot for the uptake of N₂O₅ on sulfuric acid aerosol: filled and open squares, wall loss before and after the aerosol experiment; filled circles, loss in the presence of aerosol particles. Data shown for 40% RH at 298 K. Aerosol surface area per volume of gas = 0.085 m⁻¹. Errors shown are estimated from the noise in the measured signal.

TABLE 2: Reactive Uptake Coefficients Measured at Each Relative Humidity at 298 K^a

RH (%)	[H ₂ SO ₄] (wt %)	γ_{av}	no. of determinations
8	64.5 ± 1.7	0.035 ± 0.007	4
10	64.5 ± 1.7	0.039 ± 0.007	2
22	57.0 ± 1.1	0.041 ± 0.007	4
30	52.9 ± 1.1	0.030 ± 0.004	13
40	47.8 ± 1.0	0.028 ± 0.008	5
50	43.1 ± 0.9	0.040 ± 0.006	4
70	33.2 ± 0.9	0.039 ± 0.005	5
80	26.3 ± 1.5	0.028 ± 0.013	6
8–80	26.3–64.5	0.033 ± 0.004	43

^a Stated errors on the mean γ at 95% confidence level. Errors on H₂SO₄ wt % result from a ±2% error in the relative humidity measurement.

complete form derived by Fuchs and Sutugin.¹¹ The radius used in the calculation is at the peak of the measured surface area distribution. However, since the contribution of the diffusion factor ($a/D_{\text{N}_2\text{O}_5}$) is small, the reactive uptake coefficient did not significantly change when a was varied. For the low-temperature work the diffusion coefficients were calculated using the formula of Lovejoy and Hanson¹² (eq 2).

$$D_{\text{N}_2\text{O}_5} = \frac{63.92}{(P/\text{Torr})} \left(\frac{T/K}{293} \right)^{1.94} \quad (2)$$

Result and Discussion

Kinetics of N₂O₅ Uptake. A typical plot showing the result of a kinetic run is shown in Figure 2. From this plot it is apparent that the rate of N₂O₅ loss is significantly greater in the presence of aerosol than in its absence. Second, the decay of N₂O₅ is exponential as expected for a first-order loss reaction. The first-order decay constant was then corrected according to the procedure above. From the corrected decay rate coefficients the uptake coefficients, γ , were calculated using eq 1 for each set of experimental conditions. Using this procedure, γ for the reaction of N₂O₅ was determined over a range of relative humidities from 8 to 80% or H₂SO₄ concentrations of 26.3–64.5 wt %. The results are shown in Table 2 and plotted in Figure 3. The data points shown have been obtained from a number of determinations at each relative humidity as shown in the table. The results are quite reproducible, as shown by the small error which is the standard deviation on the mean of the stated number of experiments at the 95% confidence level.

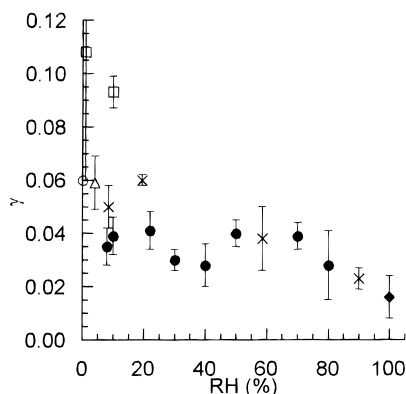


Figure 3. Uptake coefficient of N₂O₅ on aqueous sulfuric acid solutions as a function of relative humidity at 298 K: filled circles, this work; crosses, Hu and Abbatt;⁴ triangles, Lovejoy and Hanson;¹² open circles, Fried et al.;¹³ squares, Mozurkewich and Calvert;¹⁶ diamond, George et al.²⁵ Errors shown for this work are at the 95% confidence level of the average of a number of determinations.

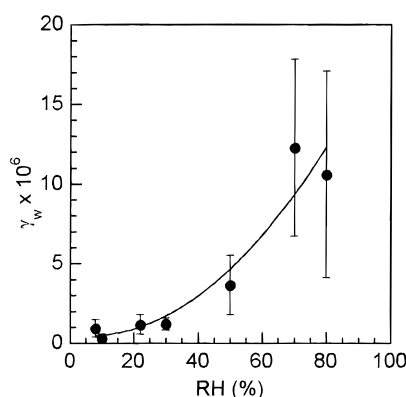


Figure 4. Observed wall loss (plotted as γ_{wall}) as a function of relative humidity. The shown line is a quadratic polynomial fit to the data. Errors shown are at the 95% confidence level of the average of a number of determinations.

Room temperature literature values are shown in Figure 3 for comparison. The uptake coefficients agree well with those recently reported by Lovejoy and Hanson¹² and Fried et al.,¹³ both of which were measured on small aerosol particles. Our data are also consistent with the results presented by Van Doren et al.¹⁴ for the uptake on large (60 μm) droplets of water and strong acid and the work of Kirchner et al.¹⁵ using a liquid water jet. The uptake coefficients presented by Hu and Abbatt⁴ agree numerically quite well with our data, but the apparent influence of relative humidity on the uptake coefficient hinted in their work was not found in our measurements. The results of Mozurkewich and Calvert¹⁶ do not agree with the other data, although it should be noted that this was the first attempt to measure the uptake coefficient of N₂O₅ on sulfuric acid aerosol and the errors were very large. Their results were in fact superseded by new measurements from the same laboratory published by Fried et al.¹³

The observed wall loss, k_w , at 298 K was found to increase with increasing relative humidity. Values of the uptake coefficient on the wall, γ_w , are shown in Figure 4. These data were calculated from the measured wall loss corrected for diffusion,¹⁰ k_w , using eq 3, where r is the radius of the flow tube and ω is the mean molecular speed.

$$\gamma_w = 2k_w r / \omega \quad (3)$$

The plot shows the uptake on the wall of the flow tube increases with relative humidity up to approximately 70% at

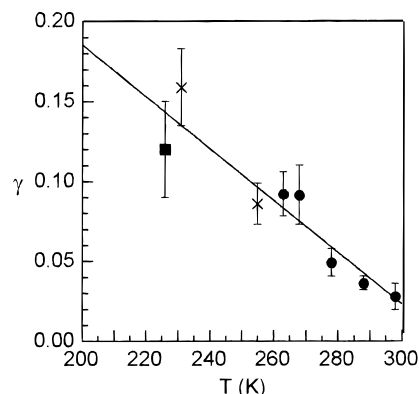


Figure 5. Uptake coefficient for N₂O₅ on sulfuric acid aqueous solutions as a function of temperature at 40% RH: filled circles, this work; crosses, Robinson et al.;⁵ filled square, Hanson and Ravishankara.¹⁸ Errors shown for this work are at the 95% confidence level of the average of a number of determinations.

TABLE 3: Reactive Uptake Coefficients Measured at Different Temperatures at 40% Relative Humidity^a

temp (K)	[H ₂ SO ₄] (wt %)	γ_{av}	$\gamma_{\text{wall}} (\times 10^6)$	no. of determinations
298	47.8	0.028 ± 0.008	2.78 ± 1.02	5
288	47.7	0.036 ± 0.004	1.45 ± 0.08	4
278	44.3	0.049 ± 0.009	10.40 ± 2.13	3
268	42.2	0.091 ± 0.019	6.64 ± 1.34	2
263	42.1	0.092 ± 0.013	7.56 ± 1.53	3

^a Stated errors are at 95% confidence level.

which point no further increase is apparent, although the reproducibility in this region is poor. This observed behavior could be due to the build up of a surface layer of water on the interior wall of the flow tube, which increases in extent with relative humidity. The magnitude of γ_w at low humidity is small, as expected for a nonpolar surface, i.e. the halocarbon wax coating. The end of the exponential increase at $\sim 70\%$ humidity could be due to the fact that above this point the liquid film is extensive enough that the amount of water present to absorb the N₂O₅ on the wall is no longer the factor limiting the rate of wall loss. The measured γ_w is significantly smaller at low RH than the value of $\gamma_w > 6 \times 10^{-6}$ reported by Hanson and Lovejoy¹⁷ for uptake on the glass surface of their flow tube at low relative humidity. At moderate humidities the wall loss reported in their work is comparable with our measurements. Similar behavior has been observed by George et al.²⁵ in their study of the uptake of N₂O₅ on NaCl solutions.

Temperature Dependence of N₂O₅ Uptake. The reactive uptake coefficients were measured over the temperature range 263–298 K at a fixed relative humidity of 40%, corresponding to an acid strength of about 45 wt %. From the results shown in Figure 5 and Table 3 it is apparent that the uptake coefficient shows a negative temperature dependence. These data are consistent with the low-temperature data presented by Robinson et al.⁵ for uptake on large droplets, and the work of Hanson and Ravishankara,¹⁸ which are also plotted in Figure 5. The temperature dependence of the wall loss, presented in Table 3, is less pronounced and less reproducible and depends on the history of the flow tube wall.

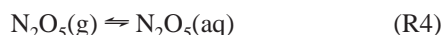
Mechanism of N₂O₅ Hydrolysis. The overall uptake of a reactive gas into liquid droplets that are small enough to avoid gas diffusion limitations can be expressed in terms of the mass accommodation coefficient α , and the liquid-phase reactivity, γ_{react} , using the resistance equation (e.g. see Schwartz¹⁹ and Davidovits et al.²⁰)

$$\frac{1}{\gamma} = \frac{1}{\alpha} + \frac{1}{\gamma_{\text{reacn}} + \gamma_{\text{soln}}} \quad (4)$$

where

$$\gamma_{\text{reacn}} = (4H^*RT/\bar{c})[D_e k_{\text{reacn}}]^{1/2} \quad (5)$$

Here H^* is the effective Henry's coefficient for trace gas solubility, D_e the liquid-phase diffusion coefficient, \bar{c} the molecular velocity, and k_{reacn} the liquid-phase reaction rate coefficient. In our analysis we have assumed that the solubility limitation to the uptake rate, $\gamma_{\text{sol.}}$, can be ignored. If the liquid-phase reaction rate is fast, the uptake rate is controlled by accommodation at the surface, i.e., reaction R4. On the other hand if the reaction rate is slow, the liquid-phase reaction rate controls reactive uptake.



Consideration of the temperature dependence of γ offers a way of distinguishing which controlling processes operate at the liquid interface. The process of accommodation at the liquid interface has been described in terms of a thermodynamic model for uptake (Davidovits et al.²⁰ and reviewed by Nathanson et al.²¹). In this theory the incoming molecule has to pass through a sharp but finite transition region several molecular diameters in thickness within which the density increases from the gas to the liquid phase. This model uses the concept that this narrow region is a dense gaslike state in which nucleation around the incoming molecule is constantly occurring. The equilibrium density of clusters containing N molecules is proportional to $\exp(-\Delta G_N/RT)$ where ΔG_N is the molar Gibbs energy for the formation of a cluster with N molecules. ΔG_N increases with cluster size, reaches a maximum, and then decreases. This implies that clusters smaller than a certain critical size evaporate whereas clusters larger than this serve as condensation centers, grow in size and become part of the bulk liquid. Davidovits et al.²⁰ suggest that gas uptake proceeds via the growth of critical clusters; i.e. if the incoming gas molecule is a part of a critical cluster, it becomes adsorbed into the solution. The temperature dependence of α , or γ if the uptake is accommodation controlled, is expressed in terms of the free energy for accommodation, $\Delta G_{\text{obs}}^\ddagger$, i.e. the Gibbs energy of the transition state between the gas phase and the aqueous phase solvation.

$$\frac{\alpha}{1-\alpha} = \exp\left(\frac{-\Delta G_{\text{obs}}^\ddagger}{RT}\right) \quad (6)$$

Since $\Delta G^\ddagger = \Delta H^\ddagger - T\Delta S^\ddagger$ the values for enthalpy and entropy for accommodation of N_2O_5 , ΔH_{obs} and ΔS_{obs} , can be obtained by plotting $\ln[\gamma/(1-\gamma)]$ vs $1/T$. Figure 6 shows a plot of the measured data, at 45 and 70 wt % H_2SO_4 , as well as the data for uptake on pure water reported by George et al.²⁵ according to eq 6. The values for ΔH_{obs} and ΔS_{obs} obtained from the gradient and the intercept are shown in Table 4. These results fit very well with the data for a wide range of compounds presented by Davidovits et al.,²⁰ which show a linear correlation between ΔH_{obs} and ΔS_{obs} for accommodation into liquids. Thus the observed temperature dependence is consistent with mass accommodation control for reactive uptake of N_2O_5 . From the theory presented by Davidovits et al.,²⁰ the average number of molecules, N , required to form a critical cluster large enough to ensure uptake of the N_2O_5 can be calculated using the obtained values of ΔH_{obs} and ΔS_{obs} , respectively (eqs 7 and 8);²⁰ these cluster sizes are also shown in Table 4.

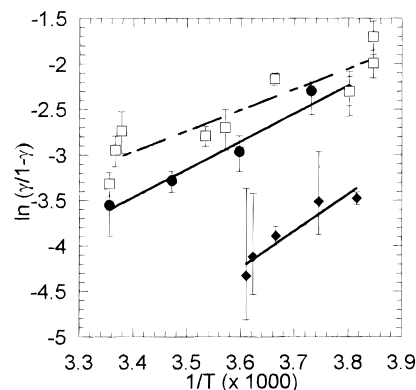


Figure 6. Plot of $\ln[\gamma/(1-\gamma)]$ vs $1/T$. The gradient of this plot gives $-\Delta H/R$ and the intercept $\Delta S/R$: filled circles, our data at ca. 45 wt % acid; squares, literature data for ca. 70 wt % acid;^{4,5,13,14,17} diamonds, data for uptake of N_2O_5 on water reported by George et al.²⁵ Errors shown for this work are at the 95% confidence level of the average of a number of determinations.

TABLE 4: Enthalpies, Entropies and Critical Cluster Sizes

H_2SO_4 (wt %)	ΔH_{obs} (kJ/mol)	ΔS_{obs} (J/K/mol)	N (from ΔH_{obs})	N (from ΔS_{obs})
70	-18.9 ± 7.6	-103 ± 39	1.88	1.82
45	-25.0 ± 8.4	-115 ± 30	2.09	2.14
0	-33.5 ± 18.5	-156 ± 78	2.39	2.54

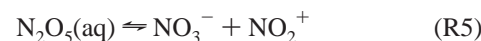
^a N = average number of molecules in a critical cluster.

$$\Delta H = -41.8(N-1) + 31.48(N^{2/3}-1) \quad \text{kJ mol}^{-1} \quad (7)$$

$$\Delta S = -123.31(N-1) + 38.5(N^{2/3}-1) \quad \text{J K}^{-1} \text{mol}^{-1} \quad (8)$$

For single clusters it is obvious that the critical number must be an integer, but the observed noninteger values can be interpreted as representing the average number of molecules in critical clusters across the interfacial region. The number of molecules required to form a critical cluster with N_2O_5 is small, indicating that critical clusters form relatively easily. However, the distinct decrease in critical cluster size as the acid strength increases shows that critical clusters form more easily in strongly acidic solutions.

At lower temperatures (<260 K) both Fried et al.¹³ and Robinson et al.⁵ have shown that the temperature dependence of γ declines, and for the lowest temperatures and highest acid strengths there is a decrease in γ as temperature falls.⁵ Clearly accommodation is not rate determining under these conditions, and the liquid-phase chemistry is playing a role. This decline in γ is not very sensitive to the sulfuric acid concentration. This was explained by Mozurkewich and Calvert¹⁶ and later Fried et al.¹³ by assuming that the limiting step in the mechanism is rapid autoionization of N_2O_5 at the surface,

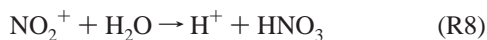


which does not involve H_2O . Alternatively, Robinson et al.⁵ suggested that two reaction channels were operating, a direct reaction with water (R6) and an additional acid-catalyzed reaction (R7) which serves to maintain the overall reaction rate as the water activity is reduced in strong acid solution.



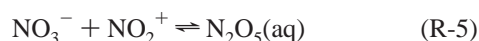
A phenomenological model based on this mechanism gave a good description of measured rates on both aerosols and bulk solutions over a fairly wide range of acid concentrations and temperatures, using a single consistent set of parameters for accommodation (α) and liquid-phase reaction (H^* , D_e , k_{reacn}).

In both the mechanisms of Fried et al.¹³ and Robinson et al.,⁵ HNO₃ is eventually produced via reaction R8 and/or R9.



The two mechanisms both involve formation of NO₂⁺, as an intermediate species, but according to the model of Robinson et al.⁵ it is only produced at high H⁺ activity, i.e. in strong acid. Although this extensive model has been tested over a range of conditions for acid particles, it is apparently inconsistent with the formation of NO₂⁺ proposed by Behnke et al.²² in the reaction of N₂O₅ with Cl⁻ in neutral sodium chloride aerosol particles. They observed ClNO₂ as the main product from the N₂O₅ reaction and suggested that it was due to the reaction between Cl⁻ and NO₂⁺ in the aqueous phase. This mechanism was later supported by the results of Schweitzer et al.²³ for the reaction between N₂O₅ and aqueous sodium halide droplets at temperatures down to 262 K. However, they observed only a weak temperature dependence of the measured uptake coefficients on dilute salt droplets, in contrast to our measurements on acid aerosols. They concluded that the uptake of N₂O₅ on dilute NaCl, NaBr, and NaI solutions are not accommodation limited and that liquid-phase processes control the uptake rate.

Wahner et al.³ measured the rate of uptake of N₂O₅ on sodium nitrate particles and found that the uptake coefficient decreased significantly with increased concentration of NO₃⁻ in the aerosol. This inhibiting effect was attributed to the reaction between NO₂⁺ and NO₃⁻, reforming N₂O₅ in competition with the hydrolysis of NO₂⁺.



If reaction R5 is an important step in the hydrolysis mechanism, the reverse reaction R-5 may affect the uptake coefficients measured in the present study if nitric acid (as NO₃⁻) builds up in the particles over the course of an experiment. To determine if this was the case, the maximum concentrations of nitric acid that could be present in the aerosol resulting from N₂O₅ hydrolysis was compared with the measured uptake coefficient. No correlation was found between nitric acid concentration and the rate of uptake, which implies either that inhibition does not occur or that the nitric acid formed quickly degasses from the aerosol particles as the aerosol has a very low pH. This is in agreement with the results of Hanson²⁴ who has shown that the uptake coefficient for N₂O₅ at low temperatures (200–230 K) only depends slightly on the HNO₃ concentration, i.e. a change of around 20% on going from 0 to 15 wt % HNO₃. In addition, the solubility of HNO₃ in acid solutions at higher temperatures is limited.

From the above discussion we conclude that all three initial reactions R5–R7 of N₂O₅(aq) are plausible and that heterogeneous dissociation is dominant at room temperature in accordance with the studies of Behnke et al.,²² Schweitzer et al.,²³ and Wahner et al.³ Under these conditions the accommodation of N₂O₅ is the rate determining step in strong acid solution. At lower temperatures, i.e. below 260 K, an important role for the acid-catalyzed reaction R7, as proposed by Robinson et al.,⁵ is needed to account for the absence of a dependence of the uptake

coefficient as the water activity falls in strong acid solution. If the compensating effect of reactions R6 and R7 is the explanation of the observed behavior at low temperatures, it must be concluded that the importance of the autoionization of N₂O₅, reaction R3, is diminished at low temperatures.

Atmospheric Implications. The work presented in this paper has provided new data for the uptake and hydrolysis of N₂O₅ on sulfuric acid aerosols. Reliable data are now available for the reactive uptake coefficient of this reaction over the range of temperatures, acid strength, and relative humidity expected in the troposphere and the stratosphere.

Our results show that for modeling the global troposphere ($T > 260$ K) a value of $\gamma(\text{N}_2\text{O}_5 + \text{H}_2\text{O})$ between 0.03 and 0.1 should be used depending on temperature. Dentener and Crutzen¹ assumed a value of 0.1 for the uptake coefficient of N₂O₅ on ammonium hydrogen sulfate aerosol in their tropospheric model. However, from a sensitivity study they showed that this reaction still has an extremely important effect on the oxidizing capacity of the troposphere even with a value as low as $\gamma = 0.01$. The effect of including heterogeneous chemistry in their model with $\gamma = 0.1$ gave decreases in NO_x, O₃, and OH by 49, 9, and 9%, respectively, compared to a base case with no heterogeneous chemistry. Using the lower reactivity of $\gamma = 0.01$, the decreases in NO_x, O₃, and OH were still significant, i.e. 40, 4, and 3%.

Conclusion

N₂O₅ reacts with water in sulfuric acid aerosol particles to form HNO₃. At 298 K the reaction probability is 0.033 ± 0.004 and is independent of relative humidity in the range 8–80%. The lack of relative humidity dependence of the uptake coefficient is consistent with possible mechanisms suggested in the literature.

The reactive uptake coefficient for N₂O₅ on submicron sulfuric acid aerosol shows a negative temperature dependence in the range 263–298 K, which is consistent with the higher values of γ reported earlier for lower temperatures. The temperature dependence data fit well with the thermodynamic model presented by Davidovits et al.²⁰ and Nathanson et al.,²¹ reproducing the correlation between observed ΔH and ΔS for the uptake process.

This reaction has an important effect on the oxidizing capacity of the troposphere, as suggested by the model of Dentener and Crutzen¹. When the reaction is included in their mathematical model of the atmosphere, it leads to a significant decrease in the tropospheric concentrations of NO_x, ozone, and OH and gives better agreement between the model and measurements of the concentrations of these species.

Acknowledgment. We gratefully acknowledge the loan of equipment from Dr. David Ames and Dr. Kevin Clemitshaw. This work was supported by the EU environment project "HECONOS" (Contract No. ENV4-C797-0407) and by the U.K. NERC (Contract No. GST/02/1884). D.J.S. thanks the U.K. NERC for the award of a studentship.

References and Notes

- (1) Dentener, F. J.; Crutzen, P. J. *J. Geophys. Res.* **1993**, *98*, 7149.
- (2) Fahey, D. W.; Kawa, S. R.; Woodbridge, E. L.; Tin, P.; Wilson, J. C.; Jonsson, H. H.; Dye, J. E.; Baumgardner, D.; Borrmann, S.; Toohey, D. W.; Avallone, L. M.; Proffitt, M. H.; Margitan, J.; Loewenstein, M.; Podolske, J. R.; Salawitch, R. J.; Wofsy, S. C.; Ko, M. K. W.; Anderson, D. E.; Schoeberl, M. R.; Chan, K. R. *Nature* **1993**, *336*, 509.
- (3) Wahner, A.; Mentel, T. F.; Sohn, M.; Stier, J. *J. Geophys. Res.* **1998**, *103*, 31103.
- (4) Hu, J. H.; Abbatt, J. P. D. *J. Phys. Chem.* **1997**, *101*, 871.

- (5) Robinson, G. N.; Worsnop, D. R.; Jayne, J. T.; Kolb, C. E.; Davidovits, P. *J. Geophys. Res.* **1997**, *102*, 3583.
- (6) Baker, J.; Ashbourn, S. F. M.; Cox, R. A. *Phys. Chem. Chem. Phys.* **1999**, *1*, 683.
- (7) Perry, R. H.; Green, D. W. *Perry's Chemical Engineers' Handbook*, 7th ed.; McGraw-Hill: New York, 1997; Section 2.
- (8) Fahey, D. W.; Eubank, C. S.; Hubler, G.; Fehsenfeld, F. C. *Atmos. Environ.* **1985**, *19*, 1883.
- (9) Keyser, L. F. *J. Phys. Chem.* **1984**, *88*, 4750.
- (10) Brown, R. L. *J. Res. Natl. Bur. Stand.* **1978**, *83*, 1.
- (11) Fuchs, N. A.; Sutugin, A. G. *Highly Dispersed Aerosols*; Ann Arbor Science: Ann Arbor, MI, 1970.
- (12) Lovejoy, E. R.; Hanson, D. R. *J. Phys. Chem.* **1995**, *99*, 2080.
- (13) Fried, A.; Henry, B. E.; Calvert, J. G.; Mozurkewich, M. *J. Geophys. Res.* **1994**, *99*, 3517.
- (14) Van Doren, J. M.; Watson, L. R.; Davidovits, P.; Worsnop, D. R.; Zahniser, M. S.; Kolb, C. E. *J. Phys. Chem.* **1991**, *95*, 1684.
- (15) Kirchner, W.; Welter, F.; Bongartz, A.; Kames, J.; Schweighoeffer, S.; Schurath, U. *J. Atmos. Chem.* **1990**, *10*, 427.
- (16) Mozurkewich, M.; Calvert, J. G. *J. Geophys. Res.* **1988**, *93*, 15889.
- (17) Hanson, D. R.; Lovejoy, E. R. *Geophys. Res. Lett.* **1995**, *22*, 1493.
- (18) Hanson, D. R.; Ravishankara, A. R. *J. Geophys. Res.* **1991**, *96*, 17307.
- (19) Schwartz, S. E. In *Chemistry of Multiphase Atmospheric Systems*; Jaeschke, W., Ed.; NATO ASI Series; Springer-Verlag: Berlin, 1986; p 415.
- (20) Davidovits, P.; Hu, J. H.; Worsnop, D. R.; Zahniser, M. S.; Kolb, C. E. *J. Chem. Soc., Faraday Discuss.* **1995**, *100*, 65.
- (21) Nathanson, G. M.; Davidovits, P.; Worsnop, D. R.; Kolb, C. E. *J. Phys. Chem.* **1996**, *100*, 13007.
- (22) Behnke, W.; George, C.; Scheer, V.; Zetzsch, C. *J. Geophys. Res.* **1997**, *102*, 3795.
- (23) Schweitzer, F.; Mirabel, P.; George, C. *J. Phys. Chem.* **1998**, *102*, 3942.
- (24) Hanson, D. R. *Geophys. Res. Lett.* **1997**, *24*, 1087.
- (25) George, C.; Ponche, J. L.; Mirabel, P.; Behnke, W.; Scheer, V.; Zetzsch, C. *J. Phys. Chem.* **1994**, *98*, 8780.